JOURNAL OF MATERIALS SCIENCE 9 (1974) 175–183

Cleavage step deformation in brittle solids

M. V. SWAIN, B. R. LAWN
School of Physics, University of New South Wales, Kensington, New South Wales 2033, Australia

S. J. BURNS
Department of Mechanical and Aerospace Sciences, University of Rochester, Rochester, New York, USA

The nature and origin of sub-surface deformation associated with steps on cleavage surfaces of brittle solids is investigated. The geometrical configuration of step formation during cleavage is first discussed in terms of an interaction between crack segments propagating on adjacent planes. Observations of cleavage surfaces, using optical microscopy, scanning electron microscopy, and X-ray topography, are then described. It is concluded that the cleavage steps form primarily according to a mechanism in which adjacent crack segments first overlap to produce a connecting cleavage sliver, and subsequently join at one end (sometimes both ends) of the sliver to complete the separation of the cleavage halves. The slivers close in imperfect registry with the underlying parent material, thereby leaving a residual gap or dislocation network beneath the undercut steps. This mechanism is in accord with previous observations of step-associated deformation, hitherto taken as evidence of local plasticity.

1. Introduction

The atomically flat cleavage is an ideal that is rarely approached in the fracture of brittle solids. In the vast majority of cases cleavage faces exhibit a complex pattern of surface markings, which may be regarded as a visual record of disturbances suffered by the propagating crack [1]. In favourable instances quantitative information on crack positions and velocities may be read from the pattern. Again, in the case of small, incomplete fractures, observations of the behaviour of interfacial structure during crack closure may be directly related to the question of reversibility in crack growth [2]. Further, since local disturbances must inevitably enhance the already intense stress concentration at the tip of a propagating crack, surface markings become favoured sites for sub-surface deformation during fracture: the state of a fresh cleavage surface may, therefore, act as a pointer to the subsidiary deformation properties of a brittle solid.

This paper is concerned with the mechanical properties of the most prevalent of all surface markings, the cleavage step. In particular, attention is focused on the stress state which prevails during step formation. A theoretical model, derived from proposals put forward by earlier workers, is first developed in an attempt to predict the geometrical configuration of the cleavage step. Experimental observations on the cleavage of several highly brittle solids, including diamond-structured crystals, glass, zinc and lithium fluoride, are then presented in support of the model. It will be argued that secondary fracture is the dominant mode of attendant sub-surface deformation during step formation, contrary to the assertion of some previous investigators. The relevance of these conclusions to deformation-sensitive properties of materials is an important adjunct of this work.

2. Mechanism of cleavage step formation

Cleavage steps form when a crack front advances through a solid on more than one plane. As the material separates across the fracture interface the adjacent crack planes join up to produce a stepped crack profile. The steps thus formed lie closely parallel to the direction of main crack propagation. In a general description of the

process one needs to specify (i) the origin of crack-front disturbance, and (ii) the manner in which material separates at the "riser" of the step. Of these two aspects only the second is directly pertinent to the present study: the first aspect will accordingly be dealt with relatively briefly.

2.1. Origin of crack-front disturbance

Among the better-known mechanisms responsible for departures from atomically smooth fracture are the following:

(a) the main crack may form by the coalescence of a number of smaller cracks initiating from non-coplanar sources;

(b) a crack approaching its terminal velocity will tend to "bifurcate" onto adjacent planes [3];

(c) an originally smooth crack experiencing a shear stress parallel to its front will tend to accommodate the disturbance by segmenting into partial fronts separated by "lance-like" steps [4, 5]. (In this way the crack plane orients itself normal to the direction of maximum tension);

(d) a cleavage crack in a crystal suffers a twist on intersecting a grain boundary, and thereby segments as in case (c) [6]. On a smaller scale, the crack front intersecting atomic-scale defects, such as screw dislocations [7], tends to produce microsteps which subsequently amalgamate into "river patterns" of macroscopic steps [8].

2.2. Step-separation mechanism

The manner in which material separates at a cleavage step requires a close look at the interaction between advancing cracks on neighbouring planes. Friedel [8] has pointed out that the creation of a cleavage step locally impedes the crack front as depicted schematically in Fig. 1. This is to be expected, particularly for large steps, since all separation mechanisms will require the expenditure of extra fracture energy, if only to create new surface area at the step riser. Thus, the cleavage step must form at some distance behind the main crack front, so the cracks on adjacent planes can be considered to approach each other from mutually opposing directions transverse to the main crack front. This point shows the way to a simple model for a stress analysis.

We choose to represent the interacting cleavage cracks as mutually opposed edge cracks in a large tensile specimen. To our knowledge no exact solution is available for this problem, but an approximate, and physically instructive,

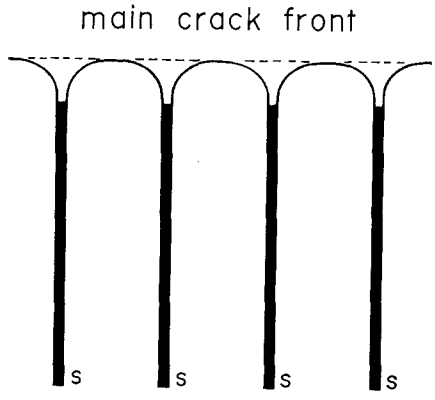

Figure 1 Schematic representation of cleavage-step pinning of main crack front. Broken line indicates position of a hypothetical uninterrupted front, full lines indicate crack segments on adjacent planes. S denotes stepped regions linking the adjacent segments.

"fracture mechanics" analysis [9] may be carried out by assuming the pre-existence of a single crack, 1, and considering the growth of a second crack, 2, in the field of 1. Fig. 2a shows the system: here the unprimed co-ordinates refer to an origin at the tip of crack 1 and the primed co-ordinates refer to an origin at the mouth of crack 2; the subscript c indicates the tip position of crack 2. The separation distance between crack planes is taken to be small compared with crack lengths ($y_c \ll x_c'$), so that any changes in stress intensity in the vicinity of closely approaching crack tips may be ascribed wholly to the interaction between fields.

The local stress field about the tip of crack 1 in the absence of crack 2 has tensile and shear components [9]

$$\left.\begin{aligned} \sigma_{yy} &= \frac{K_{I_0}}{(2\pi r)^{\frac{1}{2}}} \cos\frac{\theta}{2}\left(1 + \sin\frac{\theta}{2}\sin\frac{3\theta}{2}\right) \\ \sigma_{xy} &= \frac{K_{I_0}}{(2\pi r)^{\frac{1}{2}}} \sin\frac{\theta}{2}\cos\frac{\theta}{2}\cos\frac{3\theta}{2} \end{aligned}\right\} \quad (1)$$

where the stress-intensity factor K_{I_0} relates the intensity of the field to the applied tensile loading. Fig. 2b shows the distribution of stresses $\sigma(x, y_c)$ along the ultimate path of crack 2. It is evident that the tensile component dominates the shear component in the prior field through which crack 2 is to propagate.

Now suppose we introduce the second crack. Stress-intensity factors for this crack may be computed for each of the prior stress com-

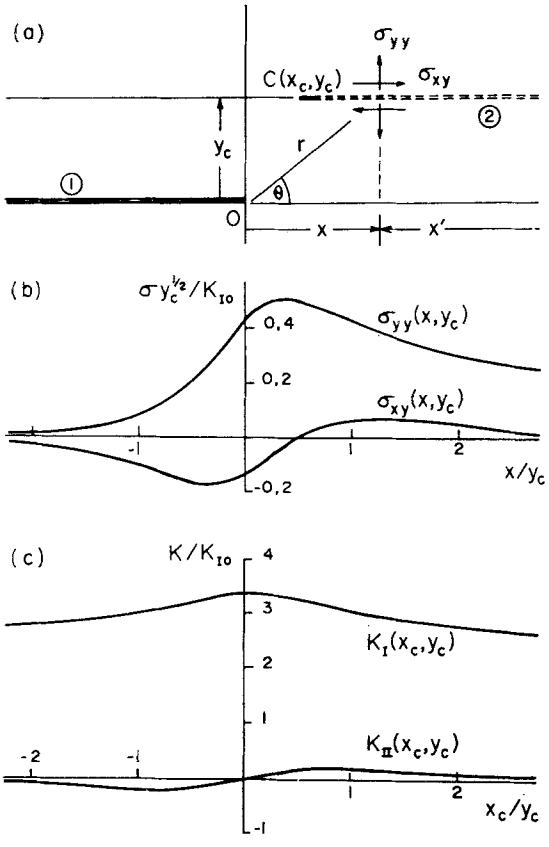

Figure 2 Mutually opposed edge cracks in tensile loading. (a) Crack 1 pre-existent at tip position 0; crack 2 at tip position C advances through field of 1. (b) Local stress field of crack 1 along ultimate path of crack 2. (c) Stress-intensity factors for crack 2 as function of tip-separation co-ordinate x_c.

ponents from standard formulae [9]; in terms of primed co-ordinates we have

$$\left.\begin{aligned} K_I &= \int_0^{x_c'} \frac{2\sigma_{yy}(x', y_c')}{\pi^{\frac{1}{2}}} \left(\frac{x_c'}{x_c'^2 - x'^2}\right)^{\frac{1}{2}} dx' + K_{I0} \\ K_{II} &= \int_0^{x_c'} \frac{2\sigma_{xy}(x', y_c')}{\pi^{\frac{1}{2}}} \left(\frac{x'_c}{x_c'^2 - x'^2}\right)^{\frac{1}{2}} dx' \end{aligned}\right\} \quad (2)$$

The term K_{I_0} in the first of these expressions appears as the limiting value in the case of zero interaction*. A convenient transformation in co-ordinates may be made by means of the connecting equation

$$x + x' = x_c + x_c'; \quad (3)$$

in the approximation of large cracks, Equation 2 reduces to

$$\left.\begin{aligned} K_I &\simeq \left(\frac{2}{\pi}\right)^{\frac{1}{2}} \int_{x_c}^{\infty} \frac{\sigma_{yy}(x, y_c)dx}{(x - x_c)^{\frac{1}{2}}} + K_{I_0} \\ K_{II} &\simeq \left(\frac{2}{\pi}\right)^{\frac{1}{2}} \int_{x_c}^{\infty} \frac{\sigma_{xy}(x, y_c)dx}{(x - x_c)^{\frac{1}{2}}} \end{aligned}\right\} \quad (4)$$

Values of $K(x_c, y_c)$ obtained by substituting Equation 1 into Equation 4 and integrating numerically are shown in Fig. 2c.

The stress-intensity factors provide a useful guide to the behaviour of the mutually approaching edge cracks. First, they indicate the magnitude of the interaction. Here the dominant term is clearly K_I, the factor associated with the tensile mode of crack propagation. Fig. 2c shows a substantial reinforcement of the stress intensity as the cracks approach and overlap. Thus we may conclude that opposing edge cracks will exert a strong mutual attraction favouring a pronounced overlap configuration.

Second, the stress-intensity factors indicate the direction of the interaction. Up to this point we have, of course, implicitly assumed that the opposing cracks suffer no deviation from their respective planes. Now, it is well known that cracks tend to align themselves normal to the direction of greatest tension. For a plane crack entering a region of shear this tendency will manifest itself as a gradual deflection of the fracture trajectory: in terms of crack 2 in Fig. 2 the deflection with respect to crack 1 will be initially repulsive and then attractive upon mutual approach. However, semi-quantitative considerations suggest that any such crack-plane disturbance will be of minor significance. Erdogan and Sih [10] have demonstrated that crack deflection goes with the ratio K_{II}/K_I; typically, at ratio unity the deflection is of order one radian, yet in Fig. 2c the greatest ratio attained is 0.06. In crystalline solids this apparent reluctance of the cracks to deviate much from their parallel-plane geometry may be further enhanced by preferred-cleavage tendencies.

We now have only to explain the manner in which the adjacent cracks link up to enable the cleavage halves to separate as the main crack front progresses. Three possible sequences are illustrated in Fig. 3; in each case the main crack front is advancing into the page.

Case (a). The adjacent cracks deflect towards each other and link up at their tips. This mechanism has been proposed for germanium cleavage [11]. However, our conclusion above concerning

*Strictly, these expressions apply only to a single plane crack in an infinite, isotropic medium, and may be suspect when crack overlap is large.

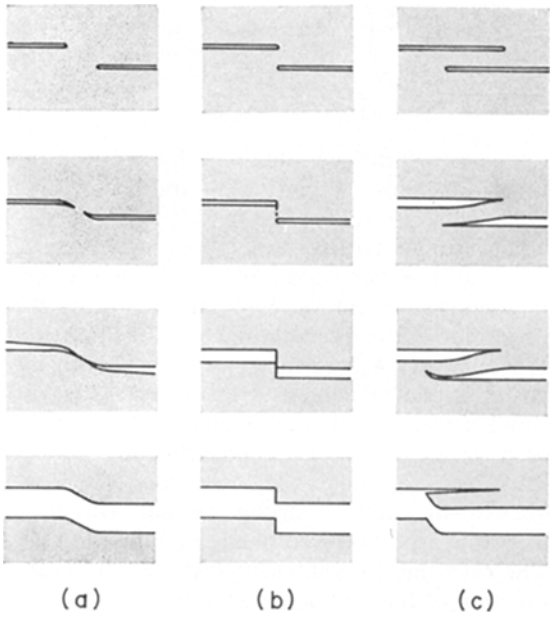

Figure 3 Three possible modes of cleavage step formation, shown in four stages of crack propagation. Main crack advancing into page. (a) Adjacent cracks attract and merge tip-to-tip. (b) Shear failure occurs to form orthogonal step. (c) Cracks overlap and merge tip-to-plane.

the reluctance of approaching cracks to deviate towards each other would appear to rule out this possibility.

Case (b). The adjacent cracks link up orthogonally at the point of overlap. Here again our analysis favours continued extension of the cracks into an overlap configuration. On the other hand, the shear stress across the region of crack-tip separation must be appreciable; thus for a solid intrinsically weak in shear an orthogonal step might be expected to form via a slip mode of failure. Gilman [12] proposed such a mechanism to account for the near-orthogonal cleavage steps shown by rocksalt-type crystals with {100} cleavages. However, highly brittle solids are, by necessity, relatively strong in shear [13]; moreover, the step geometry shown by rocksalt-type crystals is not inconsistent with the separation mode (c) below.

Case (c). The adjacent cracks first overlap and then link up as the tip of one crack intersects the plane of the other. In the large-overlap configuration, the analysis embodied in Fig. 2 loses much of its credibility, for the resulting sliver of material connecting the separating cleavage halves behaves more as a double-ended cantilever than as a portion of material adjacent to an isolated edge crack in an infinite specimen. As the main crack front advances further into the page, the connecting sliver becomes subjected to an increasing bending moment, especially in the base regions, until a critical breaking point is reached. This mechanism, first conceived by Orowan [14], has been identified in several brittle cleavages [5, 6, 15-17].

3. Observations of cleavage steps

Experimental observations have been made of steps on a wide range of cleavage surfaces. In preparing cleavage specimens our main aim was to produce surfaces with a few well-formed, widely spaced steps so that any subsidiary deformation could be observed without complication. Such specimens could be prepared simply by tapping a chisel into a notched slab oriented for "easy cleavage". Several "model" materials, materials with well-documented fracture properties and with particular amenability to examination by certain microscopic techniques, were investigated.

3.1. Optical and scanning electron microscopy

The topography of the fresh cleavage surfaces was initially surveyed by optical microscopy. All materials showed essentially the same basic features in the step patterns, although crystallographic tendencies were more apparent in crystals with greater cleavage anisotropy. Surface areas of particular interest were earmarked for observation in the scanning electron microscope. A few cleaved specimens were etched prior to examination in an attempt to delineate any outcropping regions of sub-surface deformation.

In a search for definitive evidence for any one step-separation mechanism, two observations stood out. Both confirmed the crack-overlap model (c) in Fig. 3 above. The most direct evidence was obtained by viewing transparent specimens (glass, LiF) in normally incident light. At some of the larger steps Fizeau interference fringes were clearly visible, as in Fig. 4. These fringe patterns indicate the presence of residual wedge-shaped gaps between undercut steps and parent material. From the patterns the wedge angle of the gaps was estimated to vary between 0.1 and 1.5°, with an average value of 0.5°. The usefulness of the Fizeau patterns was limited to only those larger steps whose residual gap separation exceeded that necessary to

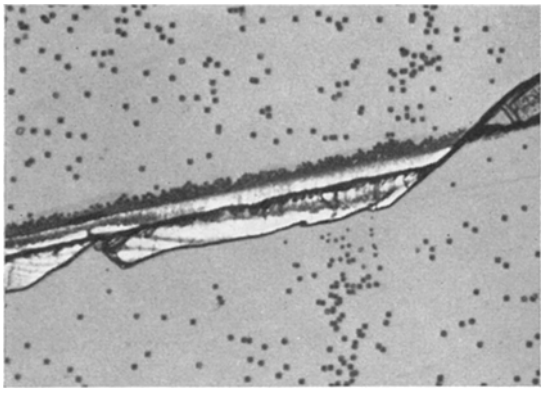

Figure 4 Optical micrograph (normally reflected green light) of (001) cleavage in LiF. Surface has been etched. Note interference fringes at undercut step, ceasing at point of upward deflection of step at right. Note also high density of dislocation etch pits at base region of step (randomly scattered pits indicate grown-in dislocations). Lower portion of micrograph corresponds to lower-level side of step. Width of field 0.6 mm.

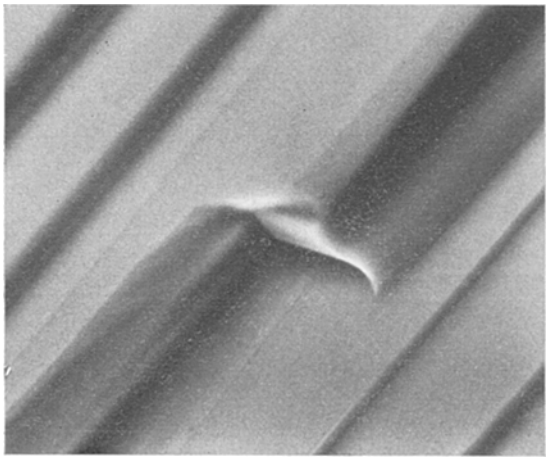

Figure 5 Scanning electron micrograph of steps on (111) Si cleavage surface. Note abrupt discontinuity at undercut step. Width of field 85 μm.

produce a single interference fringe, namely one half-wavelength of light.

The second observation pointing to the crack-overlap model presented itself in the form of discontinuities in geometry along the length of the steps. An example is shown in Fig. 5, a scanning electron micrograph of a silicon cleavage surface. Discontinuities of this kind were a common feature of all fracture surfaces examined. Their occurrence could be satisfactorily explained only in terms of a deflection in the base fracture of the near-symmetrical connecting sliver in Fig. 3c from one end to the other. Such a deflection would require only a small disturbance in stress conditions at the advancing crack front. The step geometry resulting from the proposed mechanism is depicted schematically in Fig. 6. Thus on deflection of the step from the A-A to the B-B configuration, residual undercutting should abruptly cease on the lower cleavage surface (thereby explaining the absence of fringes at extreme right in Fig. 4) and simultaneously reappear on the upper surface. Observations by other workers [6, 16] substantiate this prediction. In the special event that the stress field fluctuations prove insufficient to disturb the essential symmetry of the configuration in Fig. 3c, the sliver would presumably fracture simultaneously at both ends, in which case no residual undercutting would be evident on either fracture face. This picture is consistent with the invariable presence of microscopic "cleavage whiskers" and other debris on fresh cleavage surfaces [15]. Fig. 7 shows a clear example of a partly dislodged fragment of undercut step on a cleavage surface of silicon.

Those specimens subjected to an etch treatment showed distinctive signs of preferential chemical attack in the stepped regions. Again, this is in accord with the undercutting hypothesis, since imperfect mating between overlapping sliver and parent block inevitably leaves the surrounding material in a state of residual elastic strain. Of the materials surveyed, namely diamond-type crystals, glass, zinc and lithium fluoride, only the last showed any evidence for the operation of subsiduary deformation modes other than the secondary fracture described above. In lithium fluoride, bands of dislocation etch pits were observed at the larger overlapping cleavage slivers (Fig. 4). This is not an unexpected result, for rocksalt-type crystals are known to have a slightly plastic cleavage [6, 7, 16, 18-20]. However, plasticity mechanisms have also been positively identified in zinc cleavages [21], and tentatively in the remaining materials cited: we cannot discount the possibility that deformation resulting from such mechanisms never intersects the cleavage surface, and thereby remains inaccessible to the etchant.

3.2. X-ray diffraction microscopy (topography)

A powerful, non-destructive technique for

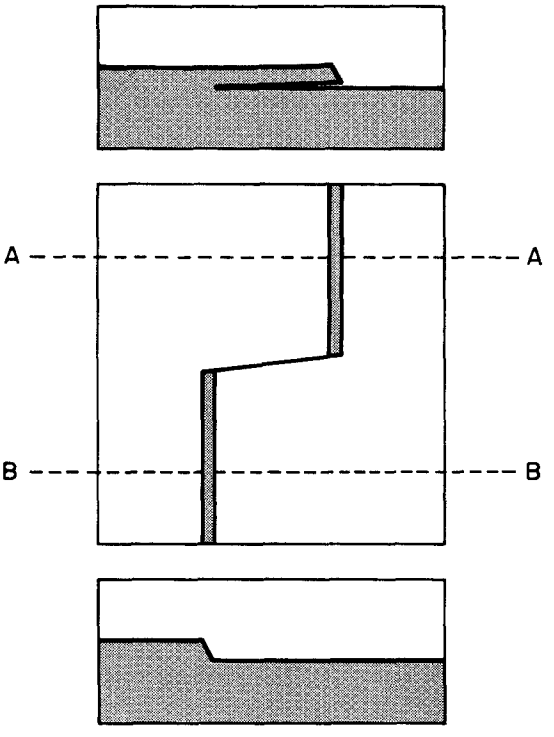

Figure 6 Schematic of cleavage step-deflection mechanism. Centre diagram represents surface view of lower cleavage face. Upper and lower diagrams represent section views through A-A and B-B respectively. Note undercutting at section A-A only. (Upper cleavage face would have complementary geometry, except in the case of sliver detachment at both ends.)

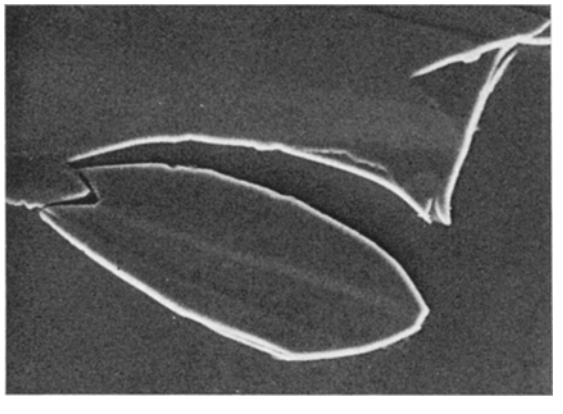

Figure 7 Scanning electron micrograph of detail at step region on a (111) Si cleavage surface. Note partially dislodged sliver fragment. Width of field 0.6 mm.

studying the imperfection content of nearly perfect crystals is that of X-ray diffraction topography. Both transmission [22] and reflection [23] variants of this technique have proved useful in identifying cleavage-generated dislocations in lithium fluoride [18, 20] and zinc [21]. In the present work attention was directed toward silicon, although a few further topographs were taken of other crystals with particularly favourable step patterns. The advantage of working with silicon is that single crystals are readily available in near-perfect form; any diffraction contrast on the topographs could, therefore, be attributed unambiguously to the cleavage process itself. Moreover, the question of whether plastic flow accompanies cleavage step formation in diamond-type crystals is a contentious issue which bears on device technology, as we shall indicate later.

The best diffraction contrast was obtained in transmission topographs of specimens thinned down to about 300 μm. The thinning procedure involved coating the cleavage surface with protective lacquer (later removed by solvent) and polishing away the back surface by mechanical and chemical means. Most crystals prepared in this manner showed slight non-uniformities in thickness, as evidenced by the appearance of broad, faint "Pendellösung" (equal thickness) fringes [24]. Of course, with reflection topographs, no such specimen preparation was necessary.

Strong diffraction contrast was observed at cleavage steps in all topographs. Lesser contrast appeared at locations where debris lay on the cleavage surface. These features are seen in the transmission topographs of silicon in Figs. 8 and 9. The step contrast is characteristic of residual elastic strain, pointing once more to the undercutting model. Furthermore, the occurrence of image discontinuities along the lengths of a majority of the steps lends strong support to the step-deflection mechanism of Fig. 6: these abrupt changes in image contrast (seen to best advantage in Fig. 8) correlate well with step deflections observed in the optical microscope.

A close examination of fine details in the diffraction micrographs of several silicon cleavage surfaces revealed no trace of any contrast that might be associated with dislocation images. Some faint transverse striations were occasionally noted at step risers where an overlapping sliver had been torn away with the opposing cleavage face (Fig. 8): optical microscopy of the corresponding surface areas disclosed fine arrays of transverse sub-markings, themselves step-like in appearance. Again, in two

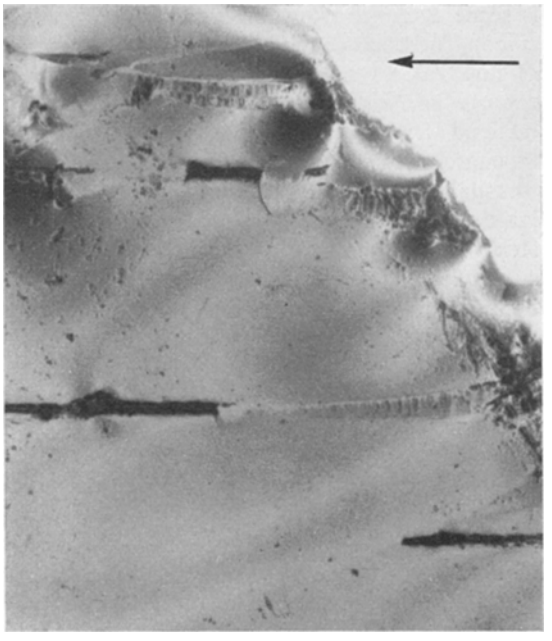

Figure 8 Transmission X-ray topograph of (111) Si cleavage, showing some particularly large steps. Note transverse striations in regions of weak step contrast. Heavy damage at top-right edge was caused by mechanical polishing during specimen preparation. AgKα radiation, $\bar{2}20$ diffraction vector. Width of field 10 mm.

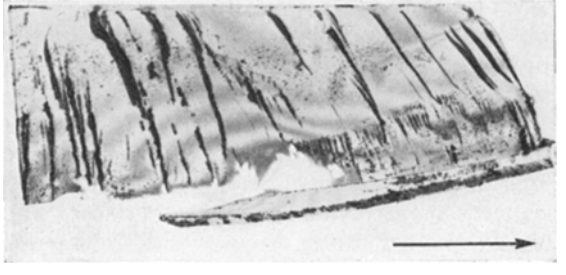

Figure 9 Transmission X-ray topograph of (111) Si cleavage. Note lateral displacement of Pendellösung fringe contours at some of the larger steps. Ag$K\alpha$ radiation, $0\bar{2}0$ diffraction vector. Length of arrow 4 mm.

isolated cases fringe patterns, with characteristic spacing less than 10 μm, were faintly visible in undercut step regions where the associated residual strain was unusually slight. On the other hand, with zinc, cleavage-induced dislocation arrays parallel to the basal cleavage plane [21] were invariably observed beneath steps: Fig. 10, a reflection topograph, is an example. Thus from the X-ray evidence, together with the null etch results, one might be led to conclude that silicon is indeed truly brittle, zinc only partially so.

However, the fine scale of the above topographic detail lies close to the limit of resolution of X-ray microscopy, namely $\approx$ 2 μm. It would, therefore, seem logical to supplement the X-ray study by means of high-resolution transmission electron microscopy. Here we may conveniently draw on the proliferation of electron microscopy observations in the literature.

Figure 10 Reflection X-ray topograph of (0001) Zn cleavage. Note dislocation array at undercut step SS. Lower portion of micrograph corresponds to lower-level side of step. Co$K\alpha$ radiation, $(1\bar{1}.03)$ diffraction vector. Width of field 0.65 mm.

4. Discussion

Our observations suggest that the crack-overlap mechanism of step separation is widespread, if not predominant, in brittle solids, at least for steps on a macroscopic scale. In accordance with this model, residual sub-surface strain may be associated with imperfect closure and healing at the interface between overlapping sliver and underlying parent block. The failure of opposing faces to key together in perfect registry is not uncommon in the closure of small-scale fractures [2]. The presence of minute sub-markings (e.g. transverse striations in Fig. 8) and fracture debris may be responsible for substantial residual-gap wedge angles; for instance, micrometre-scale disturbances account for the wedge angle of order one degree in Fig. 4. In the diamond-structure crystals the gap displacements appear to be accommodated entirely by elastic strain in the surrounding material, whereas in lithium fluoride and zinc there is evidence for accompanying dislocation mechanisms. These conclusions are, of course, pertinent only to room temperature observations; at elevated

temperatures plasticity is likely to become a dominant factor in the cleavage of all solids.

With these points in mind it is interesting to review the interpretations made by earlier workers in transmission electron microscopy studies. Fringe patterns and dislocation networks on the sub-micrometre scale have been observed beneath steps on cleavage surfaces of silicon [25] and germanium [26], magnesium oxide [27], zircon [28], and graphite [29]. In all cases, the sub-surface patterns were confined to an interface lying parallel to the cleavage surface and terminating at the step riser. The consensus of opinion is that such observations constitute evidence for a glide mechanism. However, in the diamond-structure crystals, the weight of existing evidence on dislocation motion argues heavily against even small-scale glide at room temperature; only at elevated temperatures does the Peierls stress drop significantly below the theoretical shear strength for the ideal diamond lattice [30]. Moreover, in magnesium oxide the (001) plane of cleavage (hence the plane of the sub-surface interface) does not even correspond to a favoured slip plane.

The step-undercutting model outlined in the present study suggests an alternative explanation of the interfacial patterns. Imperfect closure between sliver and underlying parent crystal would cause a small mismatch between the lattice planes in the two crystal portions. On the reasonable assumption that the residual bending in the sliver produces a mutual tilting rather than dilation of the lattice planes, we may predict the generation of a rotation Moiré pattern, by diffraction contrast, in both X-ray and electron micrographs*. Now the fringe spacing in rotation Moirés is given by $D = d/\theta$, where d is the spacing of diffracting planes and θ is the angular mismatch. Taking $d \simeq 0.2$ nm as a typical value, and $\theta \simeq 0.5°$ corresponding to the average residual-gap wedge angle cited in Section 3.1 as an upper limit to the lattice tilt, we obtain $D \simeq 25$ nm as a lower-limit estimate of the fringe spacing. This is consistent with the scale of the fringe patterns observed in the electron microscope. For the same type of pattern to be resolvable by the X-ray method, however, the angular mismatch would need to be at least two orders of magnitude smaller than the above value. There is some evidence from the X-ray topography of silicon, for instance the present isolated sightings of step fringe systems (Section 3.2) and previous reports of widely-spaced Moirés at surface-inclined fractures [2], that sufficiently small mismatch may eventuate under conditions of unusually favourable geometry. The relatively large average mismatches in the present cleavage step observations are no doubt attributable to the susceptibility of the thin overlapping slivers to bending: if, on the other hand, the sub-markings at the interface between sliver and underlying crystal were by chance to key together at isolated points along a step, a high degree of closure might be attained in local areas.

The appearance of dislocations rather than Moiré fringes in some of the micrographs would then follow naturally if, in the course of breakage of the sliver, substantial interfacial recontact were to occur beneath the undercut step. Energy considerations would favour relaxation of the system into an interfacial dislocation array, with regions of "restored" crystal between the dislocations [31], provided the chemical bonds remained unsaturated during the separation process†. Mismatch dislocations have been previously proposed in connection with crack healing in sodium chloride [32, 33]. The dislocation array beneath the cleavage step in the zinc topograph of Fig. 10, and an earlier observation of a "fringe system" made under near-identical conditions [34], may well fall within this category [35, 36].

Finally, mention may be made of a twinning mode proposed to explain the presence of spurious reflections in X-ray diffraction spot patterns of germanium cleavage surfaces [37]. While we can neither support nor refute this possible deformation mode in the diamond-type crystals, it may be worth pointing out that no markings which might be identified with twins were evident in our observations, or in the electron microscopy observations referred to above.

5. Concluding remarks

The crack-overlap model described here presents a consistent picture of cleavage step mechanics in brittle solids. It not only emphasizes the basic role of secondary fracture in the cleavage pro-

*Without specific knowledge of the diffraction vectors for those published electron micrographs which show apparent Moiré fringe patterns we cannot rigorously confirm the dominance of a rotational component, despite the direct evidence in the micrographs themselves that the material at the cleavage steps is tilted.
†As, for example, in a dynamic cleavage in which environmental contaminants have insufficient time to penetrate into the advancing fissures.

cess, but also demonstrates the need for extreme caution in the interpretation of associated deformation patterns. Such considerations are of particular concern in connection with the general deformation properties of highly brittle materials, e.g. diamond-type crystals and glassy solids: these materials always fracture in the linear stress-strain region in conventional testing arrangements, for it is no simple matter to avoid a component of tension in any loading system other than in an elaborate high-pressure apparatus. Consequently, much of the evidence for room-temperature plasticity in highly brittle materials has derived from somewhat fortuitous observations of subsidiary deformation at cleavage steps, indentation sites, etc. Our present analysis seriously questions the cleavage step evidence, and a similar state of controversy is currently arising over the indentation evidence. In the diamond-structure materials the precise nature of the subsidiary deformation has aroused intense interest because of a strong correlation between semiconducting properties and surface conditions [38]: the potential control of such conditions in device technology clearly requires a basic understanding of the underlying mechanisms.

Acknowledgements

We wish to thank J. S. Williams for discussions. We are grateful to the School of Textile Technology at the University of New South Wales for making their scanning electron microscope available to us. Financial assistance from an Australian Commonwealth Scholarship is also acknowledged (M. V. Swain).

References

1. C. A. ZAPFFE and C. O. WORDEN, *Acta Cryst.* **2** (1949) 377, 383, 386.
2. J. S. WILLIAMS, B. R. LAWN and M. V. SWAIN, *Phys. Stat. Sol. (a)* **2** (1970) 7.
3. E. YOFFE, *Phil. Mag.* **42** (1951) 739.
4. A. SMEKAL, *Oesterr. Ing. Arch.* **7** (1953) 49.
5. E. SOMMER, *Eng. Fract. Mech.* **1** (1969) 539.
6. F. F. LANGE, *Phil. Mag.* **16** (1967) 761.
7. J. J. GILMAN, *Trans. Met. Soc. AIME* **203** (1955) 1252.
8. J. FRIEDEL, "Fracture" (Eds. B. L. Averbach, D. K. Felbeck, G. T. Hahn and D. A. Thomas) (Wiley, New York, 1959) p. 498.
9. P. C. PARIS and G. C. SIH, "Fracture Toughness Testing and its Applications" (ASTM Special Technical Publication No. 381, 1965) p. 30.
10. F. ERDOGAN and G. C. SIH, *J. Basic Eng.* **85** (1963) 519.
11. D. HANEMAN and E. N. PUGH, *J. Appl. Phys.* **34** (1963) 2269.
12. J. J. GILMAN, *ibid* **27** (1956) 1262.
13. A. KELLY, W. R. TYSON and A. H. COTTRELL, *Phil. Mag.* **15** (1967) 567.
14. E. OROWAN, "Dislocations in Metals" (AIME, New York, 1954) p. 144.
15. J. D. VENABLES, *J. Appl. Phys.* **31** (1960) 1503.
16. F. F. LANGE and K. A. D. LAMBE, *Phil. Mag.* **18** (1968) 129.
17. R. B. LEONESIO, *Eng. Fract. Mech.* **1** (1968) 237.
18. C. T. FORWOOD and B. R. LAWN, *Phil. Mag.* **13** (1966) 595.
19. V. SCHMIDT, "Proceedings of Conference on Yield and Fracture" (Inst. Physics and Phys. Soc., London, 1966) p. 24.
20. S. J. BURNS and W. W. WEBB, *Trans. Met. Soc. AIME* **236** (1966) 1165.
21. S. J. BURNS, *Acta Metallurgica* **18** (1970) 969.
22. A. R. LANG, *J. Appl. Phys.* **30** (1959) 1748.
23. J. B. NEWKIRK, *Trans. Met. Soc. AIME* **215** (1958) 483.
24. N. KATO and A. R. LANG, *Acta Cryst.* **12** (1959) 787.
25. D. R. FRANKL, *J. Appl. Phys.* **34** (1963) 3514.
26. W. P. NOBLE and H. K. HENISCH, *ibid* **38** (1967) 2472.
27. M. H. LEWIS, *Phil. Mag.* **13** (1966) 1123.
28. L. A. BURSILL and A. C. MCLAREN, *J. Appl. Phys.* **36** (1965) 2084.
29. S. AMELINCKX, "The Direct Observation of Dislocations" (Academic Press, New York, 1964) pp. 392-4.
30. H. ALEXANDER and P. HAASEN, "Solid State Physics" (Academic Press, New York, 1968) Vol. 22, p. 28.
31. S. AMELINCKX, "The Direct Observation of Dislocations" (Academic Press, New York, 1964) pp. 64-71.
32. A. J. FORTY and C. T. FORWOOD, *Trans. Brit. Ceram. Soc.* **62** (1963) 715.
33. M. P. SHASKOL'SKAYA, WANG YEN-YEN and KU SHU-CHAO, *Sov. Physics-Cryst.* **6** (1962) 483.
34. R. W. ARMSTRONG and J. M. SCHULTZ, *Acta Cryst.* **17** (1964) 1214.
35. K. S. CHANDRASEKARAN, *ibid* **19** (1965) 152.
36. A. R. LANG, *ibid* **19** (1965) 682.
37. H. SUZUKI and K. KAMADA, *J. Phys. Soc. Japan* **21** (1966) 571.
38. A. MANY, Y. GOLDSTEIN and N. B. GROVER, "Semiconductor Surfaces" (North-Holland, Amsterdam, 1965).

Received 16 July and accepted 21 August 1973.